Increasing Polymer Solar Cell Fill Factor by Trap-Filling with F4-TCNQ at Parts Per Thousand Concentration

*Han Yan, Joseph G. Manion, Mingjian Yuan, F. Pelayo García de Arquer, George R. McKeown, Serge Beaupré, Mario Leclerc, Edward H. Sargent, and Dwight S. Seferos**

The predominant challenge for all photovoltaic technologies is to minimize losses associated with recombination. Organic photovoltaics (OPVs) differ from their inorganic counterparts because of appreciable electronic disorder and significant structural heterogeneity in the OPV active layer.[1,2] These traits increase internal loss pathways known as geminate and nongeminate recombination.[3,4] In geminate recombination the electron and hole originate from the same photon, whereas in nongeminate recombination they do not. In efficient OPVs there is little geminate recombination. Nongeminate recombination losses are dominant, and they lead to a photocurrent bias dependence and a poor device fill factor (FF).[5–11]

Nongeminate recombination includes the recombination of electrons and holes (bimolecular recombination) and a trapped charge with a free charge (trap-assisted recombination).[12] Bimolecular recombination is often suppressed by optimizing charge mobility and film thickness.[13,14] Trap-assisted recombination is induced by typical OPV operating conditions (low light, low current density), and it is more difficult to remedy.[15–18] Traps can be extrinsic or intrinsic.[19] Oxygen, water, or chemical impurities are typical extrinsic traps, and are typically removed by chemical purification.[20–24] On the other hand, intrinsic traps are much more difficult to eliminate due to the inherent inhomogeneity of OPVs.[19,25]

Intrinsic charge traps arise from the energetic and structural disorder in organic semiconductors. Since the photogenerated charges originate mainly in the donor polymer, and fullerene derivatives are thought to be trap-free, most intrinsic trap-assisted recombination processes originate within the polymer.[26] Here, we describe our efforts to chemically suppress intrinsic charge traps by adding small amounts of 2,3,5,6-tetrafluoro-7,7,8,8-tetracyanoquinodimethane (F4-TCNQ). We discuss how this leads to improved photodiode performance and show that it is applicable to multiple types of polymers.

Trap-assisted recombination in a donor polymer is a two-step process (**Figure 1**a) where a hole is first trapped within the band gap and then recombines with an oppositely charged electron. Our hypothesis is that the introduction of additional carriers (i.e., dopants) will fill the states within the band gap where traps reside and thus render them electronically inert (Figure 1b). In the ground state a strong electron acceptor will induce electron transfer from the polymer to the acceptor and fill the trap states with a positively charged species. In the excited state photogenerated holes will be blocked from entering trap states and hole transport will be trap-free. The charge transfer process decreases the trap density rather than eliminating the trap states. The trap-filling mechanism is different from previous doping strategies.[27–30]

To minimize the opposing effect that counter ions may act as extrinsic traps we opted to test these hypotheses by introducing F4-TCNQ at parts-per-thousand (ppt) concentration. Specifically, the high-efficiency polymer, poly[4,8-bis(5-(2-ethylhexyl)-thiophen-2-yl)benzo[1,2-b;4,5-b′]dithiophene-2,6-diyl-alt-(4-(2-ethylhexyl)-3-fluorothieno[3,4-b]thiophene-)-2-carboxylate-2-6-diyl)] (PBDTTT-EFT) was treated with low concentrations of F4-TCNQ. Ground state electron transfer is expected to occur from the polymer to F4-TCNQ (**Figure 2**a).[31,32] The ground

Dr. H. Yan, J. G. Manion, G. R. McKeown, Prof. D. S. Seferos
Department of Chemistry
University of Toronto
80 St. George Street, Toronto, Ontario M5S 3H6, Canada
E-mail: dseferos@chem.utoronto.ca
Dr. M. Yuan, Dr. F. P. García de Arquer, Prof. E. H. Sargent
The Edward S. Rogers Department of
Electrical and Computer Engineering
University of Toronto
10 King's College Road, Toronto, Ontario M5S 3G4, Canada
Dr. S. Beaupré, Prof. M. Leclerc
Department of Chemistry
Université Laval
Avenue de la Médecine
Québec City, Québec G1V 0A6, Canada

DOI: 10.1002/adma.201601553

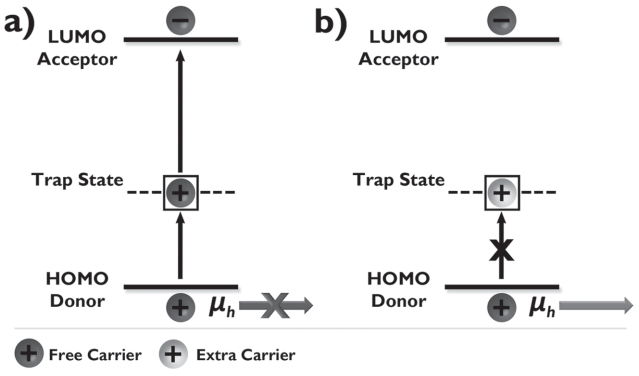

Figure 1. Models of trap-assisted recombination and trap-filling: a) Recombination between trapped holes and free electrons by a trap state; b) Trap-filling and suppression of trap-assisted recombination.

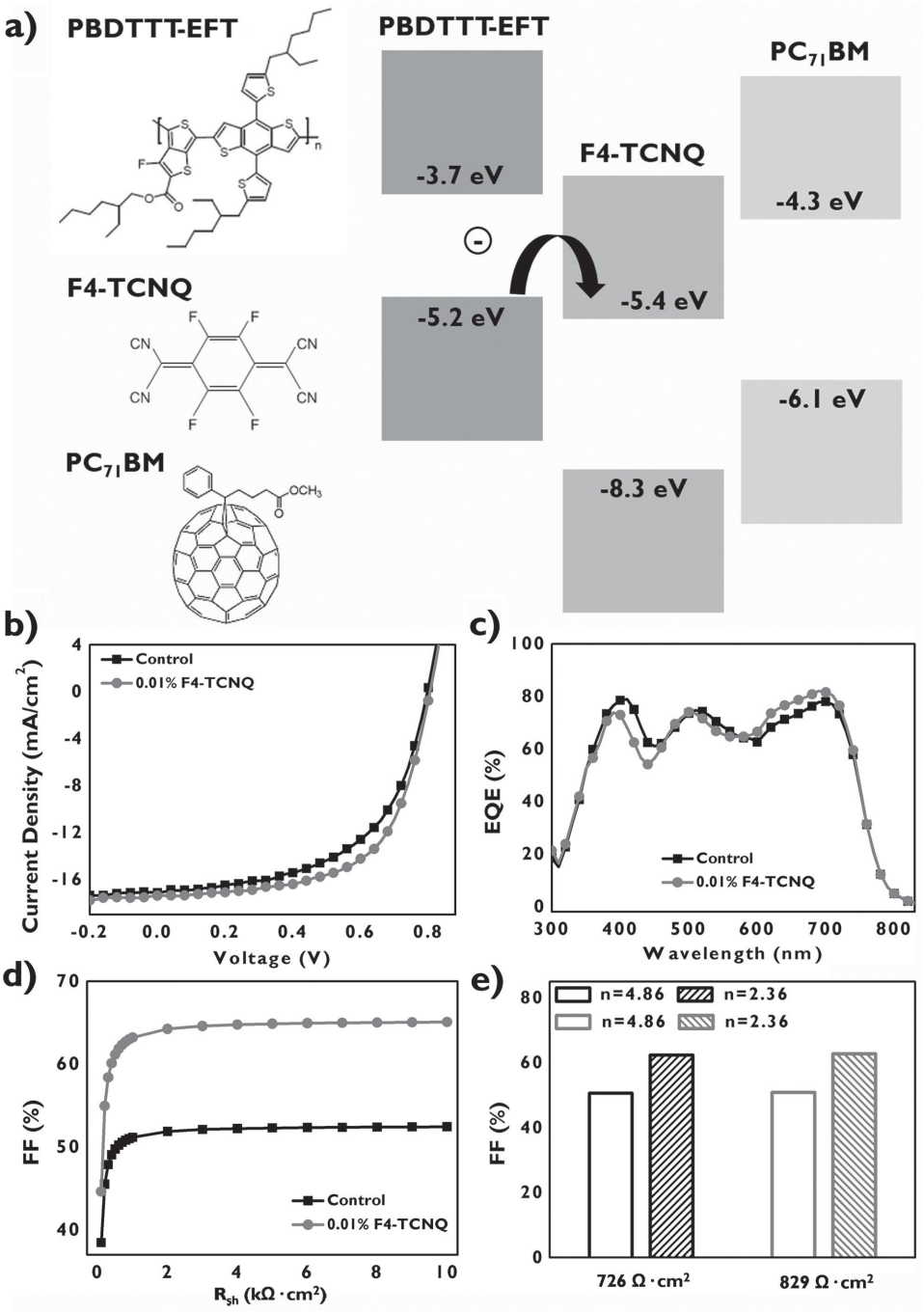

Figure 2. a) Chemical structures and energy level diagrams for PBDTTT-EFT, F4-TCNQ, and $PC_{71}BM$. The arrow depicts the charge transfer process between PBDTTT-EFT and F4-TCNQ occurring in the dark. Photovoltaic performance of PBDTTT-EFT/$PC_{71}BM$ solar cells with and without F4-TCNQ (0.01%): b) *J–V* curves; c) Corresponding EQE plots. d) FF-R_{sh} correlation with and without F4-TCNQ (0.01%). e) Histograms of FF with different *n* and R_{sh}.

state electron transfer is supported by the onset of absorption peak in infrared region and this peak is not observed with equal content of 7,7,8,8-tetracyanoquinodimethane (TCNQ) having –4.5 eV lowest unoccupied molecular orbital (LUMO) level (Figure S1 in the Supporting Information).[24] Modest photoluminescence spectrum quenching is observed by adding F4-TCNQ in neat polymer films, and we attribute this to disrupted conjugation in donor polymer by charge transfer (Figure S2 in the Supporting Information). We next fabricated photovoltaic devices to test whether this low F4-TCNQ content leads to improved device performance. Photovoltaic devices with similar film thickness (≈105 nm) were characterized in terms of short-circuit current (J_{sc}), open-circuit voltage (V_{oc}), FF, and power conversion efficiency (PCE) (**Table 1**). Interestingly, the

Adv. Mater. **2016**,
DOI: 10.1002/adma.201601553

Table 1. Photovoltaic performances of PBDTTT-EFT/$PC_{71}BM$ solar cells with various F4-TCNQ content.

Materials	J_{sc} [mA cm^{-2}]	V_{oc} [V]	FF [%]	FF_{avg} [%]	PCE_{max}[a)] [%]	PCE_{avg} [%]
Control	17.11	0.80	55.2	56 ± 1.1	7.6 [b)]	7.3 ± 0.2
0.01%	17.39	0.80	61.8	62 ± 0.5	8.6[b)]	8.2 ± 0.3
0.05%	17.71	0.80	55.5	55 ± 1.1	7.9[b)]	7.4 ± 0.2
0.1%	17.75	0.80	54.7	54 ± 1.4	7.8	7.6 ± 0.2

[a)]Average PCE of 20 devices fabricated under identical conditions ± 1 standard deviation (σ); [b)]Maximum lies outside ± 1σ (standard deviation).

lowest F4-TCNQ content (0.01%) results in the highest increase in PCE, from 7.6% to 8.6% (Figure 2b). The J_{sc} increases slightly, from 17.11 to 17.39 mA cm^{-2}, and no change in the V_{oc} (0.80 V) is observed. The most significant improvement comes from the FF, which increases from 55.2% to 61.8%. This is different from previous reports that have shown that F4-TCNQ improves device performance by increasing the J_{sc}.[33,34] To confirm our data, we measured the external quantum efficiency (EQE) to calculate the current density. We find that 0.01% doping increases the spectral response above 600 nm but decreases the response below 500 nm, leading to an almost un-changed current density of 17.18 mA cm^{-2} compared to 17.06 mA cm^{-2} for the control (Figure 2c). With further F4-TCNQ addition the PCE drops to 7.9%, and finally to 7.8% at 0.1% addition. The decay is due to decreases in FF suggesting that extra F4-TCNQ adversely affects device performance. Furthermore, the split trend of FF and J_{sc} here can be explained by the different working mechanisms of trap-filling and increased charge density.[33] We also added TCNQ instead of F4-TCNQ. Adding 0.01% TCNQ decreases the photovoltaic performances, and most notable, the FF (Figure S3 and Table S2 in the Supporting Information).

The FF is an important parameter for OPVs, however, it is currently the least understood. The observation that charge transfer improves the FF provides a means to study this parameter further. The FF is determined by the series resistance (R_s), shunt resistance (R_{sh}), and diode performance (Figure S4 in the Supporting Information).[8,35] The R_s and R_{sh} can be determined from the slope of *J–V* curve at the V_{oc} and J_{sc}, respectively, while the diode performance is determined from the ideality factor (n).[36] For control and 0.01% F4-TCNQ OPVs we find the R_s is fairly uniform (Table S1 in the Supporting Information). Moreover, differences in R_{sh} can only account for a less than 1% change in FF (Figure 2d,e; see details in the Supporting Information). Therefore n is responsible for the improved FF.

To lend more support to our proposed trap-filling mechanism we further characterized the control and F4-TCNQ devices. Small amounts of additives like 1,8-diiodooctane (DIO) and 1-chloronaphthalene can improve photovoltaic performance by optimizing film morphology. Here, we do not observe a morphology change with 0.01% F4-TCNQ or TCNQ content (Figure S5–S7 in the Supporting Information). With further addition, we observe some nanoscale aggregates in the film (Figure S8 in the Supporting Information), however this change occurs with a decrease in performance. The dark *J–V* curves indicate that 0.01% F4-TCNQ does not increase parasitic leakage current (**Figure 3**a). Under illumination the charge-transport properties require consideration of the built-in potential and the photocurrent density (J_{ph}) at low effective voltage (V_{eff}) (see details in the Supporting Information).[37] Previous studies suggest that additional charges induce charge-accumulation and decrease the built-in potential, which would suppress charge separation at donor–acceptor interfaces.[38] Here we find that the built-in potentials are the same (0.89 V) for doped and control devices. On the other hand 0.01% F4-TCNQ leads to an increase in J_{ph} at low V_{eff} (Figure 3b) and does not appear to induce new recombination pathways. Mott–Schottky plots also do not show space charge region in 0.01% F4-TCNQ devices (Figure S9 in the Supporting Information).

Trap filling should increase charge transport and decrease trap density. We examine these properties using the *J–V* curves of hole-only and electron-only devices (Figure 3c,d). Electron mobility and electron trap density are consistent in both control and 0.01% F4-TCNQ devices showing that the counter ions do not influence electron mobility or behave as electron traps. In contrast, 0.01% F4-TCNQ increases the hole mobility to a point where it balances with the electron mobility (**Table 2**). At the same time, the hole trap density decreases from a significant value to an undetectable level. Based on these results, we confirm that small amount of ground-state charge transfer fills hole traps without introducing new electronic defects. When adding 0.1% F4-TCNQ, both the hole and electron mobility decrease with increased hole and electron trap density (Table 2 and Figure S10 in the Supporting Information).

Balanced mobility decreases bimolecular recombination, while decreased trap density suppresses trap-assisted recombination. To differentiate the two recombination mechanisms we measured J_{sc} and V_{oc} as functions of light intensity (Figure S11 in the Supporting Information).[39] The J_{sc} slopes of the control and 0.01% F4-TCNQ samples are 1.04 and 1.05 (Figure 3e,f and Table 2), illustrating similar low levels of bimolecular recombination. Under open-circuit conditions, the recombination mechanism can be distinguished from the dependence of V_{oc} on the natural logarithm of the light intensity. Trap-assisted recombination has a slope of 2 kT/e, while bimolecular recombination has a slope of kT/e. We find that 0.01% F4-TCNQ decreases the slope at V_{oc} from 1.12 kT/e to 1.06 kT/e indicating suppression of trap-assisted recombination is responsible for improved FF. We also examined 0.1% F4-TCNQ in more detail (Table 2 and Figure S12 in the Supporting Information) and found that the increased slopes of J_{sc} (1.12) and V_{oc} (1.18 kT/e) are responsible for the poor FF at higher F4-TCNQ content.

Having successfully improved the relative photovoltaic performance of PBDTTT-EFT/$PC_{71}BM$ by trap filling we now test the general nature of this approach. We fabricated additional devices using statistical polyselenophene–polythiophene copolymers (P3HT-*stat*-P37S (80:20)) (inset of **Figure 4**a) and poly[*N*-9′-heptadecanyl-2,7-carbazole-alt-5,5-(4′,7′-di-2-thienyl-2′,1′,3′-benzothiadiazole)]

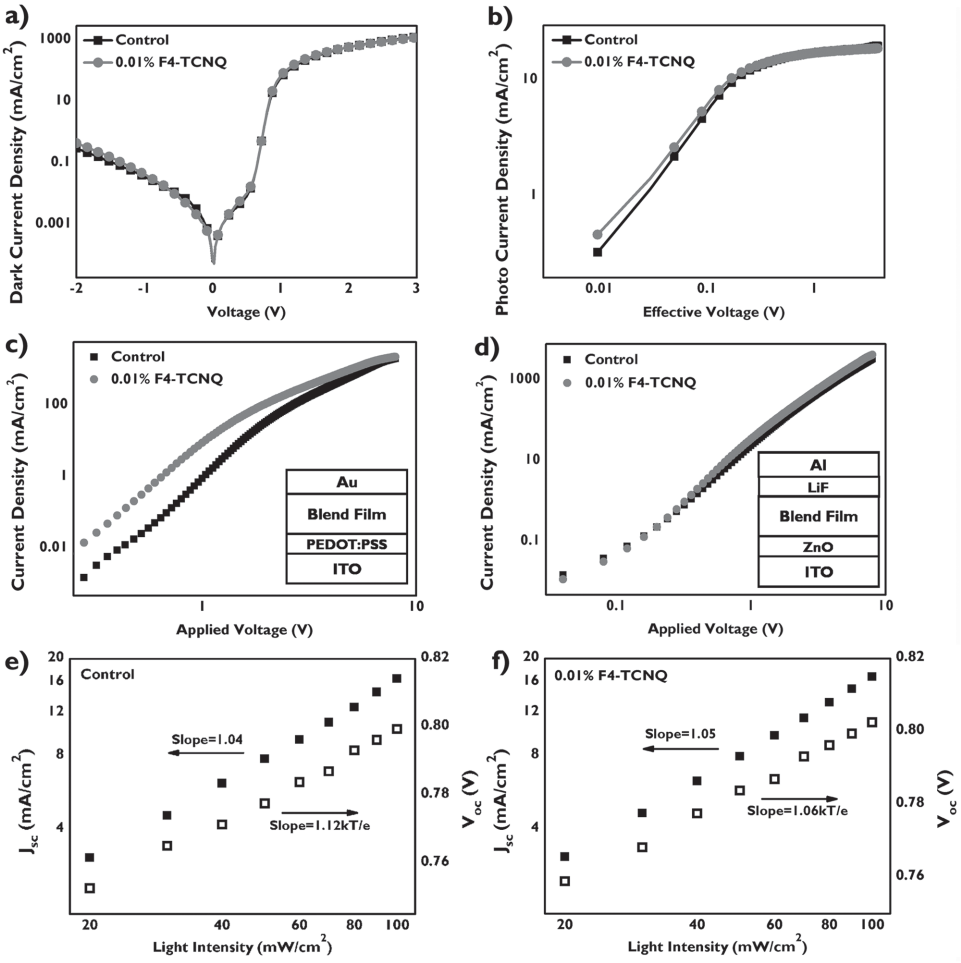

Figure 3. a,b) Dark and photo *J–V* curves of PBDTTT-EFT/$PC_{71}BM$. c,d) Hole-only and electron-only charge transport curves. e,f) Measured J_{sc} and V_{oc} of PBDTTT-EFT/$PC_{71}BM$ solar cells plotted against light intensity. The open and closed squares represent the values of V_{oc} and J_{sc} under different illumination intensities.

(PCDTBT) (inset of Figure 4c).[40–46] Selenophene-containing polymers have a low FF and thus are ideal candidates for this strategy. PCDTBT is a well-studied donor–acceptor polymer. When F4-TCNQ is added, we observe better rectifying *J–V* curves in both polymers (Figure 4a,c) without any obvious change in film morphology (Figure S13 and S14 in the Supporting Information). Consistent with results for PBDTTT-EFT, charge transfer improves PCE by increasing the FF in both cases (**Table 3** and Figure 4; see details in Table S3 and S4 in the Supporting Information).

In conclusion, we have studied the effect of ppt-level F4-TCNQ on the performance of three polymers useful for OPVs. In all cases increases in FF are observed leading to an increase in overall device performance. While adding F4-TCNQ at ppt levels does not alter active layer morphology, it modifies the electronic properties by trap-filling and this is responsible for FF improvements. We feel that these findings are important because traps are inevitable in OPVs. Further studies on other ground state electron acceptors, as well as electron donors for nonfullerene systems, may lead to significant progress in OPV performance.

Experimental Section

Materials: PBDTTT-EFT (M_n = 61 kDa, M_w = 134 kDa, $Đ$ = 2.2) was purchased from Solarmer Energy Inc. China. P3HT-*stat*-P37S (80:20) was synthesized by our group according to reported methods (M_n = 21 kDa, M_w = 26 kDa, $Đ$ = 1.3).[42–44] PCDTBT (M_n = 37 kDa, M_w = 112 kDa,

Table 2. Charge transport and recombination in PBDTTT-EFT/$PC_{71}BM$.

Materials	Hole mobility [$cm^2\ V^{-1}\ s^{-1}$]	Electron mobility [$cm^2\ V^{-1}\ s^{-1}$]	Hole/electron mobility ratio	Hole trap density [cm^{-3}]	Electron trap density [cm^{-3}]	Slope of J_{sc}	Slope of V_{oc} [kT/e]
Control	2.30×10^{-5}	1.00×10^{-4}	0.23	5.89×10^{16}	None	1.04	1.12
0.01%	1.07×10^{-4}	1.01×10^{-4}	1.06	None	None	1.05	1.06
0.1%	8.06×10^{-5}	4.97×10^{-5}	1.62	4.13×10^{16}	3.84×10^{16}	1.12	1.18

Adv. Mater. **2016**,
DOI: 10.1002/adma.201601553

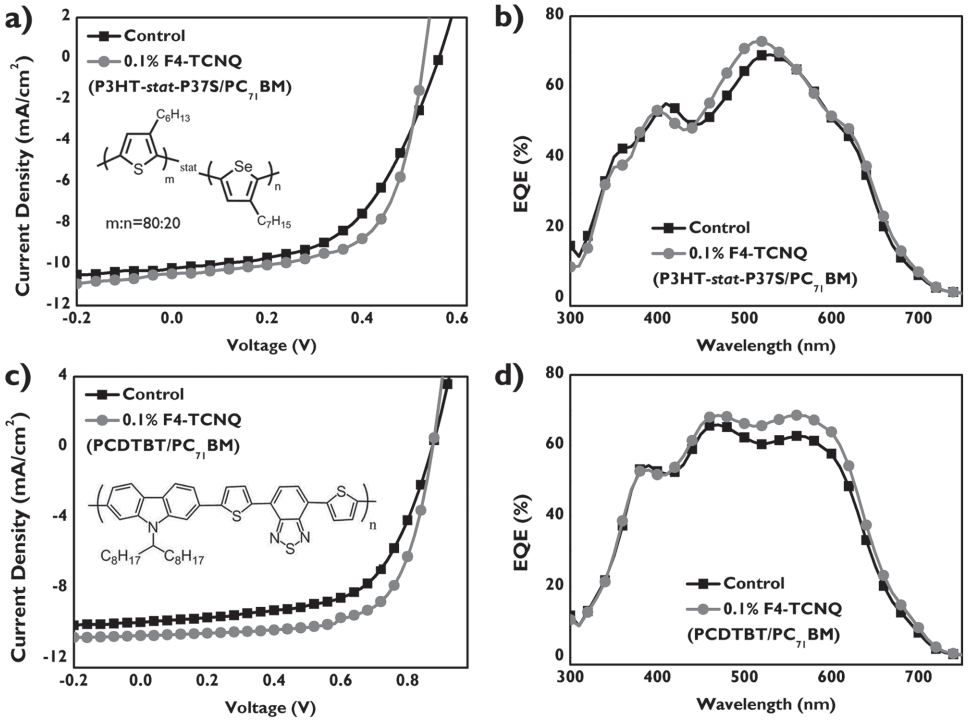

Figure 4. Photovoltaic performances of P3HT-*stat*-P37S/$PC_{71}BM$ solar cells with and without F4-TCNQ (0.1%): a) *J–V* curves; b) Corresponding EQE plots. Photovoltaic performances of P3HT-*stat*-P37S/$PC_{71}BM$ solar cells with and without F4-TCNQ (0.1%): c) *J–V* curves; d) Corresponding EQE plots.

Table 3. Photovoltaic performances of P3HT-*stat*-P37S (80:20)/$PC_{71}BM$ and PCDTBT/$PC_{71}BM$ solar cells with and without F4-TCNQ.

Materials	J_{sc} [mA cm^{-2}]	V_{oc} [V]	FF [%]	FF_{avg} [%]	PCE_{max}[a)] [%]	PCE_{avg} [%]
Control P3HT-*stat*-P37S	10.17	0.56	53.6	53 ± 1.6	3.1[b)]	2.9 ± 0.1
0.1% F4-TCNQ P3HT-*stat*-P37S	10.45	0.53	63.4	62 ± 1.7	3.5	3.4 ± 0.1
Control PCDTBT	9.93	0.87	60.2	60 ± 0.8	5.2	5.1 ± 0.1
0.1% F4-TCNQ PCDTBT	10.68	0.88	67.5[b)]	66 ± 1.0	6.3	6.2 ± 0.1

[a)]Average PCE of ten devices fabricated under identical conditions ± 1 standard deviation (σ); [b)]Maximum lies outside ± 1σ (standard deviation).

$Đ$ = 3.0) was provided by the Leclerc group.[45,46] $PC_{71}BM$ was purchased from American Dye Source. PEDOT:PSS (Clevios P VP AI 4083) was purchased from Heraeus. Zinc acetate dihydrate, ethanolamine, and 2-methoxyethanol were purchased from Sigma-Aldrich. All solvents in the experiments were used as received from Sigma-Aldrich.

Instrumentation: Gel permeation chromatography (GPC) measurements were carried out using a Malvern 350 HT-GPC system at 140 °C with 1,2,4-trichlorobenzene (stabilized with butylated hydroxytoluene). Molecular weights were determined using narrow dispersity polystyrene standards. Absorption spectra were recorded on a Varian Cary 5000 spectrometer. Photoluminescence was performed on a Photon Technology International (PTI QuantaMaster 40-F NA) spectrofluorometer with a photomultiplier detector and xenon arc lamp source. The film thickness was examined by a surface profilometer (KLA-Tencor P16+). Atomic force microscopy (AFM) imaging was carried out on a Bruker Dimension Icon microscope. Bright field transmission electron microscopy (TEM) was performed on a Hitachi H-7000 transmission electron microscopy at 100 kV accelerating voltage.

Device Fabrication and Testing: Indium-tin oxide (ITO)-coated glass substrates (Colorado Concept Coatings LLC) were cleaned successively with aqueous detergent, deionized water, methanol, and acetone for 15 min each, and then treated in an oxygen-plasma cleaner for 10 min. PEDOT:PSS was filtered through a 0.45 µm polyvinylidene fluride (PVDF) syringe filter, spin-coated at 2000 rpm, and then annealed at 150 °C for 10 min in an ambient atmosphere. PBDTTT-EFT was dissolved in chlorobenzene at concentration of 14 mg mL^{-1}. The solution was then mixed with $PC_{71}BM$ at a blend ratio of 1:1.5 with vigorous stirring at 70 °C overnight. 3% (vol%) DIO was added to solutions before use. The solar cells were fabricated by spin-coating (3000 rpm for 40 s) the active layer on PEDOT:PSS-coated ITO in a N_2-filled glove box, followed by methanol washing at 4000 rpm for 30 s. P3HT-*stat*-P37S (80:20) was dissolved in o-dichlorobenzene at concentration of 17 mg mL^{-1}, and was then mixed with $PC_{71}BM$ at a blend ratio of 1:1. The solar cells were fabricated by spin-coating at 700 rpm for 30 s, followed by thermal annealing at 150 °C for 10 min. PCDTBT was dissolved in a blend solvent of o-dichlorobenzene/chlorobenzene with blend ratio of 3:1 (vol%) at concentration of 5 mg mL^{-1}, and was then mixed with $PC_{71}BM$ at a blend ratio of 1:4. Devices were fabricated by spin-coating at 1500 rpm for 50 s, followed by thermal annealing at 70 °C for 10 min. For the devices with F4-TCNQ, different volumes of F4-TCNQ chlorobenzene solution were added in the each blend solution before spin-coating. LiF (0.8 nm) and Al (100 nm) were thermally evaporated using an

Angstrom Engineering (Kitchener, ON) Covap II metal evaporation system at 1×10^{-6} torr. The device area is 0.07 cm^2 as defined by shadow mask. *J–V* curves were obtained by a Keithley 2400 source meter under simulated AM 1.5G condition with power intensity of 100 mW cm^{-2}. The mismatch of spectrum was calibrated using Si diode with a KG-5 filter. Light-intensity dependent *J–V* curves were carried out by adjusting sample-light source distance and calibrated with the current of the Si detector. EQE measurements were recorded using a 300 W Xenon lamp with an Oriel cornerstone 260 1/4 m monochromator and compared with a Si reference cell that is traceable to the National Institute of Standards and Technology. The samples for dark and photo charge transport studies were fabricated and tested according to the same method as described for PBDTTT-EFT:PC_{71}BM solar cells. The LiF/Al was replaced with silver (200 nm) as top electrodes for the *C–V* test. *C–V* measurements were performed using an Agilent 4284A precision LCR meter under the C_p–R_p model. All measurements were performed in the dark. *C–V* sweeps were performed between −1 and +2 V with an AC signal of 1 kHz. The hole-only devices were fabricated by replacing the LiF/Al with gold (80 nm) as top electrodes, while in electron-only devices the PEDOT:PSS was replaced by zinc oxide (ZnO) as bottom electrodes. The ZnO layer was prepared by stirring 200 mg zinc acetate dihydrate and 56 mg ethanolamine in 2 mL 2-methoxyethanol at room temperature for 12 h, and spin-coating the precursors at 3000 rpm for 60 s, followed by thermal annealing at 200 °C for 1 h.

Supporting Information

Supporting Information is available from the Wiley Online Library or from the author.

Acknowledgements

This work was supported by the NSERC of Canada, The Canadian Foundation for Innovation, DuPont, and the A. P. Sloan Foundation.

Received: March 20, 2016
Revised: April 5, 2016
Published online:

[1] P. W. M. Blom, V. D. Mihailetchi, L. J. A. Koster, D. E. Markov, *Adv. Mater.* **2007**, *19*, 1551.
[2] T. M. Clarke, J. R. Durrant, *Chem. Rev.* **2010**, *110*, 6736.
[3] C. Groves, *Energy Environ. Sci.* **2013**, *6*, 3202.
[4] D. Credgington, F. C. Jamieson, B. Walker, T. Q. Nguyen, J. R. Durrant, *Adv. Mater.* **2012**, *24*, 2135.
[5] S. D. Dimitrov, J. R. Durrant, *Chem. Mater.* **2014**, *26*, 616.
[6] P. E. Keivanidis, V. Kamm, C. D. Smith, W. Zhang, F. Laquai, I. McCulloch, D. D. C. Bradley, J. Nelson, *Adv. Mater.* **2010**, *22*, 5183.
[7] D. A. Vithanage, E. Wang, Z. Wang, F. Ma, O. Inganäs, M. R. Andersson, A. Yartsev, V. Sundström, T. Pascher, *Adv. Energy Mater.* **2014**, *4*, 1301706.
[8] J. D. Servaites, M. A. Ratner, T. J. Marks, *Energy Environ. Sci.* **2011**, *4*, 4410.
[9] D. Bartesaghi, I. D. C. Pérez, J. Kniepert, S. Roland, M. Turbiez, D. Neher, L. J. A. Koster, *Nat. Commun.* **2015**, *6*, 7083.
[10] R. Mauer, I. A. Howard, F. Laquai, *J. Phys. Chem. Lett.* **2010**, *1*, 3500.
[11] W. Tress, A. Merten, M. Furno, M. Hein, K. Leo, M. Riede, *Adv. Energy Mater.* **2013**, *3*, 631.
[12] C. M. Proctor, M. Kuik, T. Q. Nguyen, *Prog. Polym. Sci.* **2013**, *38*, 1941.
[13] G. Lakhwani, A. Rao, R. H. Friend, *Annu. Rev. Phys. Chem.* **2014**, *65*, 557.
[14] T. Kirchartz, T. Agostinelli, M. Campoy-Quiles, W. Gong, J. Nelson, *J. Phys. Chem. Lett.* **2012**, *3*, 3470.
[15] C. R. McNeill, N. C. Greenham, *Appl. Phys. Lett.* **2008**, *93*, 203310.
[16] L. Tzabari, N. Tessler, *J. Appl. Phys.* **2011**, *109*, 064501.
[17] C. G. Shuttle, N. D. Treat, J. D. Douglas, J. M. J. Fréchet, M. L. Chabinyc, *Adv. Energy Mater.* **2012**, *2*, 111.
[18] R. A. Street, A. Krakaris, S. R. Cowan, *Adv. Funct. Mater.* **2012**, *22*, 4608.
[19] L. G. Kaake, P. F. Barbara, X. Y. Zhu, *J. Phys. Chem. Lett.* **2010**, *1*, 628.
[20] J. Schafferhans, A. Baumann, A. Wagenpfahl, C. Diebel, V. Dyakonov, *Org. Electron.* **2010**, *11*, 1693.
[21] H. T. Nicolai, M. Kuik, G. A. H. Wetzelaer, B. de Boer, C. Campbell, C. Risko, J. L. Brédas, P. W. M. Blom, *Nat. Mater.* **2012**, *11*, 882.
[22] S. R. Cowan, W. L. Leong, N. Banerji, G. Dennler, A. J. Heeger, *Adv. Funct. Mater.* **2011**, *21*, 3083.
[23] W. L. Leong, G. C. Welch, L. G. Kaake, C. J. Takacs, Y. Sun, G. C. Bazan, A. J. Heeger, *Chem. Sci.* **2012**, *3*, 2103.
[24] L. Kaake, X. Dang, W. L. Leong, Y. Zhang, A. J. Heeger, T. Q. Nguyen, *Adv. Mater.* **2013**, *25*, 1706.
[25] L. Lu, T. Zheng, T. Xu, D. Zhao, L. Yu, *Chem. Mater.* **2015**, *27*, 537.
[26] V. D. Mihailetchi, J. K. J. van Duren, P. W. M. Blom, J. C. Hummelen, R. A. J. Janssen, J. M. Kroon, M. T. Rispens, W. J. H. Verhees, M. M. Wienk, *Adv. Funct. Mater.* **2003**, *13*, 43.
[27] L. Lu, T. Xu, W. Chen, J. M. Lee, Z. Luo, I. H. Jung, H. I. Park, S. O. Kim, L. Yu, *Nano Lett.* **2013**, *13*, 2365.
[28] H. I. Park, S. Lee, J. M. Lee, S. A. Nam, T. Jeon, S. W. Han, S. O. Kim, *ACS Nano* **2014**, *8*, 10305.
[29] U. N. Maiti, W. J. Lee, J. M. Lee, Y. Oh, J. Y. Kim, J. E. Kim, J. Shim, T. H. Han, S. O. Kim, *Adv. Mater.* **2014**, *26*, 40.
[30] J. M. Lee, J. Lim, N. Lee, H. I. Park, K. E. Lee, T. Jeon, S. A. Nam, J. Kim, J. Shin, S. O. Kim, *Adv. Mater.* **2015**, *27*, 1519.
[31] S. Zhang, L. Ye, W. Zhao, D. Liu, H. Yao, J. Hou, *Macromolecules* **2014**, *47*, 4653.
[32] J. E. Rainbolt, P. K. Koech, E. Polikarpov, J. S. Swensen, L. Cosimbescu, A. Von Ruden, L. Wang, L. S. Sapochak, A. B. Padmaperuma, D. J. Gaspar, *J. Mater. Chem. C* **2013**, *1*, 1876.
[33] Y. Zhang, H. Zhou, J. Seifter, L. Ying, A. Mikhailovsky, A. J. Heeger, G. C. Bazan, T. Q. Nguyen, *Adv. Mater.* **2013**, *25*, 7038.
[34] A. V. Tunc, A. D. Sio, D. Riedel, F. Deschler, E. D. Como, J. Parisi, E. von Hauff, *Org. Electron.* **2012**, *13*, 290.
[35] B. Qi, J. Wang, *Phys. Chem. Chem. Phys.* **2013**, *15*, 8972.
[36] J. R. Sites, P. H. Mauk, *Sol. Cells* **1989**, *27*, 411.
[37] Q. Zhang, B. Kan, F. Liu, G. Long, X. Wan, X. Chen, Y. Zuo, W. Ni, H. Zhang, M. Li, Z. Hu, F. Huang, Y. Cao, Z. Liang, M. Zhang, T. P. Russell, Y. Chen, *Nat. Photonics* **2015**, *9*, 35.
[38] A. Liu, S. Zhao, S. B. Rim, J. Wu, M. Könemann, P. Erk, P. Peumans, *Adv. Mater.* **2008**, *20*, 1065.
[39] S. R. Cowan, A. Roy, A. J. Heeger, *Phys. Rev. B* **2010**, *82*, 245207.
[40] H. Yan, J. Hollinger, C. R. Bridges, G. R. McKeown, T. Al-Faouri, D. S. Seferos, *Chem. Mater.* **2014**, *26*, 4605.
[41] H. Yan, Y. Song, G. R. McKeown, G. D. Scholes, D. S. Seferos, *Adv. Mater.* **2015**, *27*, 3484.
[42] J. Hollinger, A. A. Jahnke, N. Coombs, D. S. Seferos, *J. Am. Chem. Soc.* **2010**, *132*, 8546.
[43] J. Hollinger, J. Sun, D. Gao, D. Karl, D. S. Seferos, *Macromol. Rapid Commun.* **2013**, *34*, 437.
[44] D. Gao, J. Hollinger, A. A. Jahnke, D. S. Seferos, *J. Mater. Chem. A* **2014**, *2*, 6058.
[45] N. Blouin, A. Michaud, M. Leclerc, *Adv. Mater.* **2007**, *19*, 2295.
[46] N. Blouin, A. Michaud, D. Gendron, S. Wakim, E. Blair, R. Neagu-Plesu, M. Belletête, G. Durocher, Y. Tao, M. Leclerc, *J. Am. Chem. Soc.* **2008**, *130*, 732.

DOI: 10.1002/adma.201601553